atmosphere

MDPI

Article

Source Apportionment of $PM_{2.5}$ in Guangzhou Based on an Approach of Combining Positive Matrix Factorization with the Bayesian Mixing Model and Radiocarbon

Tingting Li [1,2], Jun Li [1,*], Hongxing Jiang [1,2], Duohong Chen [3,*], Zheng Zong [4], Chongguo Tian [4] and Gan Zhang [1]

1 State Key Laboratory of Organic Geochemistry and Guangdong province Key Laboratory of Environmental Protection and Resources Utilization, Guangzhou Institute of Geochemistry, Chinese Academy of Sciences, Guangzhou 510640, China; litingting@gig.ac.cn (T.L.); jianghongxing15@163.com (H.J.); zhanggan@gig.ac.cn (G.Z.)
2 University of Chinese Academy of Sciences, Beijing 100049, China
3 Guangdong Environmental Monitoring Center, Guangzhou 510308, China
4 Key Laboratory of Coastal Environmental Processes and Ecological Remediation, Yantai Institute of Coastal Zone Research, Chinese Academy of Sciences, Yantai 264003, China; zzong@yic.ac.cn (Z.Z.); cgtian@yic.ac.cn (C.T.)
* Correspondence: junli@gig.ac.cn (J.L.); chenduohong@139.com (D.C.)

Received: 9 April 2020; Accepted: 14 May 2020; Published: 16 May 2020

Abstract: To accurately apportion the sources of aerosols, a combined method of positive matrix factorization (PMF) and the Bayesian mixing model was applied in this study. The PMF model was conducted to identify the sources of $PM_{2.5}$ in Guangzhou. The secondary inorganic aerosol source was one of the seven main sources in Guangzhou. Based on stable isotopes of oxygen and nitrogen ($\delta^{15}N\text{-}NO_3^-$ and $\delta^{18}O\text{-}NO_3^-$), the Bayesian mixing model was performed to apportion the source of NO_3^- to coal combustion, traffic emission and biogenic source. Then the secondary aerosol source was subdivided into three sources according to the discrepancy in source apportionment of NO_3^- between PMF and Bayesian mixing model results. After secondary aerosol assignment, the six main sources of $PM_{2.5}$ were traffic emission (30.6%), biomass burning (23.1%), coal combustion (17.7%), ship emission (14.0%), biomass boiler (9.9%) and industrial emission (4.7%). To assess the source apportionment results, fossil/non-fossil source contributions to organic carbon (OC) and element carbon (EC) inferred from ^{14}C measurements were compared with the corresponding results in the PMF model. The results showed that source distributions of EC matched well between those two methods, indicating that the PMF model captured the primary sources well. Probably because of the lack of organic molecular markers to identify the biogenic source of OC, the non-fossil source contribution to OC in PMF results was obviously lower than ^{14}C results. Thus, an indicative organic molecular tracer should be used to identify the biogenic source when accurately apportioning the sources of aerosols, especially in the region with high plant coverage or intense biomass burning.

Keywords: $PM_{2.5}$; ^{14}C; PMF model; Bayesian mixing model; primary source; secondary aerosol; Pearl River Delta (PRD)

1. Introduction

At present, air pollution, especially the high concentration of fine particulate matter ($PM_{2.5}$), is a vital environmental issue in China [1,2]. $PM_{2.5}$ pollution has adverse impacts on climate, human health and visibility, which has become a major concern of the government and public [1,3]. Clarifying the levels, characteristics, and sources of pollution were of great help to alleviate $PM_{2.5}$

pollution effectively and improve air quality [3–5]. Precise and thorough knowledge of sources and their contributions to $PM_{2.5}$ is crucial in carrying out feasible measures for controlling $PM_{2.5}$ levels. Therefore, reliable source apportionment is key to making more effective measures. The receptor model is frequently used for source apportionment of particulate matters, including chemical mass balance (CMB)[6], PMF, principal component analysis (PCA), multi-linear engine (ME-2) and Unmix [7,8]. The PMF model is one of the most widely used source apportionment methods when the sources and their profiles are unclear [8,9].

The main uncertainties of the PMF model come from the $PM_{2.5}$ collection, chemical composition measurement, col-linearity of source profile (different sources with similar profiles), and incorrect identification of secondary sources [7,10]. Secondary aerosols such as secondary sulfate and nitrate could be identified by the PMF model [2,5]. Secondary aerosol is formed primarily through atmospheric oxidation of gas precursors (e.g., volatile organic compounds (VOCs), SO_2 and NO_X), which are mainly from fossil fuel combustion, biomass burning or biogenic sources [1,11]. As a mixture of organic matter, sulfates, nitrates and ammonium, secondary aerosol has hybrid and complicated sources [1,12]. Therefore, it is always difficult to understand the sources of secondary aerosol clearly [11]. In the Bayesian mixing model, stable isotopes of nitrogen and oxygen could be applied to apportion NO_3^- sources [13]. According to the discrepancy in source apportionment of NO_3^- between the PMF and Bayesian mixing model results, nitrate in the secondary aerosol identified by PMF could be subdivided into primary sources. In 2006, Yuan et al.[14] found that secondary organic carbon (SOC) and secondary sulfate were correlated in individual seasons and had similar seasonal variation, indicating that their formation was controlled by common factors. In 2013, Huang et al.[11] also reported that secondary organic aerosol probably formed simultaneously with nitrate and sulfate in atmospheric reaction process. Assuming the sources of secondary aerosols are almost the same as those of its main components, the sources of nitrate in secondary sources were used to represent the sources of overall secondary aerosol. Hence, secondary aerosol identified by PMF also could be subdivided into primary sources according to the discrepancy in source apportionment of NO_3^- between the PMF and Bayesian mixing model results. In addition, the determination of the source numbers and the discrimination of source classes were subjective and uncertain in the PMF model [7]. Radiocarbon (^{14}C) measurements is a powerful tool to distinguish carbonaceous aerosol from fossil and non-fossil sources [15,16]. Consequently, comparing the contributions of fossil/non-fossil sources to OC and EC inferred from ^{14}C fractions with the corresponding results of PMF could assess the reliability of source apportionment results.

As one of the metropolises in southern China and the capital of Guangdong province, Guangzhou has suffered from $PM_{2.5}$ pollution with complex sources in the recent years due to many vehicles and high levels of industrialization in this area [2,5]. In the past few years, various methods were used to identify the sources of $PM_{2.5}$ in Guangzhou, including an air quality model, multivariable linear regression analysis, carbon isotopic analysis, CMB and PMF [16-19]. In this study, the PMF model was applied to apportion $PM_{2.5}$ sources using 19 chemical components. The Bayesian mixing model was performed to identify the sources of NO_3^-. ^{14}C measurement was used to assess $PM_{2.5}$ source apportionment results. Potential source contribution function (PSCF) analysis was applied to identify potential source regions of $PM_{2.5}$. The results of this study could be helpful for the design of effective $PM_{2.5}$ pollution control methods in Guangzhou.

2. Materials Methods

2.1. Sample Collection

$PM_{2.5}$ samples were collected from 16 October 2013 to 18 July 2014 in Guangzhou (23°8′ N, 113°17′ E). One month was selected every season for sampling every day (i.e., autumn: 16 October 2013–14 November 2013, winter: 21 December 2013–21 January 2014, spring: 21 March 2014–21 April 2014, summer: 21 June 2014–18 July 2014), the duration for each sample was 24 h, and finally, 92 $PM_{2.5}$ samples were collected. Fine particles were obtained on quartz fiber filters (Whatman, QM-A, 20.3 × 25.4 cm^2) preheated at 450 °C for 6 h. After sampling, the filters were wrapped with aluminum foil,

sealed in polyethylene zipper bags, and stored in a refrigerator at −20 °C. Details regarding the sampling could be found in reference [20].

2.2. Chemical Composition Analysis

Water-soluble ions (Na^+, K^+, Mg^{2+}, Ca^{2+}, NH_4^+, Cl^-, SO_4^{2-} and NO_3^-) were analyzed by ion chromatograph. Trace elements (As, Cd, Cr, Cu, Fe, Mn, Ni, Pb, V and Zn) were determined using ICP-MS (Inductively Coupled Plasma Mass Spectrometry). Portions of the filter samples (1.5 cm^2) were cut for analysis of the OC and EC contents (OC/EC) using a thermal–optical carbon analyzer (Sunset Laboratory Inc., Forest Grove, OR, USA) following a modified National Institute of Occupational Safety and Health (NIOSH) thermal–optical transmission protocol. The methods were reported by previous study [21] and details were presented in Supplementary Material Text S1.

^{14}C was measured in OC and EC to distinguish fossil and non-fossil fuel sources quantitatively. Two samples with relatively high and low $PM_{2.5}$ concentrations collected in each season were selected for ^{14}C analysis. The detailed method of ^{14}C measurement in various carbonaceous aerosols (i.e., TC, EC and water-soluble OC (WSOC)) has been described elsewhere [22,23]. The ^{14}C analysis results were expressed as fractions of modern carbon (f_M). The f_M values for OC were not measured directly but were deduced through subtraction of TC and EC based on mass balance. The detailed method and ^{14}C results were published in the previous study [24].

The nitrous oxide (N_2O) isotopic analysis method was used to quantify $\delta^{15}N\text{-}NO_3^-$ and $\delta^{18}O\text{-}NO_3^-$ for all samples [20,25]. Briefly, NO_3^- in solution was converted to N_2O, and then N_2O was used to detect $\delta^{15}N$ and $\delta^{18}O$ on an isotope ratio mass spectrometer (MAT253). The detailed method and $\delta^{15}N\text{-}NO_3^-$ and $\delta^{18}O\text{-}NO_3^-$ results were published in the previous study [20].

2.3. Source Apportionment and Performance Assessment

2.3.1. Source Apportionment Methods

The PMF model was developed by Pattero and Tapper [8,26,27]. The aims of the PMF model were to identify the suitable number of sources, the species profile of each source, and the sum of mass contributed by each source to each sample. The detailed uncertainty calculation of this method was described in Supplementary Material Text S2. In the Bayesian mixing model, stable isotopes were applied to identify the probability distribution of the source contribution to the mixture according to isotopic values and fractionation effect [20,28]. In this study, the Bayesian mixing model was utilized for determining the source of NO_3^- following the previous methods [13,20]. The details of the Bayesian mixing model are described in Supplementary Material Text S3.

2.3.2. Source Apportionment Assessment

To assess PMF model performance, the contributions of fossil/non-fossil sources to OC and EC inferred from ^{14}C measurements were compared with the corresponding results of the PMF model, respectively. The contribution fraction (R) of fossil or non-fossil sources classified in PMF results to OC and EC were calculated by Equation (1)[3]:

$$R_{ij} = \sum_{k=1}^{n} g_{ik} f_{kj} / \sum_{k=1}^{p} g_{ik} f_{kj} \quad (1)$$

where i is the specific sample, j is the species of OC or EC, n is the number of fossil or non-fossil carbon species source, p is the amount of all sources, R represents contribution fraction, g and f represent the source contributions and source profiles, respectively.

2.3.3. Sources Contribution of $PM_{2.5}$ and OC after Subdivision of Secondary Aerosol

Secondary aerosols identified by PMF could be subdivided into primary sources according to the discrepancy in source apportionment of NO_3^- between the PMF and Bayesian mixing model results.

After the secondary aerosol was subdivided, the source's contribution of $PM_{2.5}$ and OC were calculated by Equations (2–4):

$$\Delta N_s = (B_s - N_s)/N_{sa} \quad (2)$$

where *s* represent coal combustion, traffic emission and biomass burning source, B_s is the contribution fraction of *s* to NO_3^- in the Bayesian model (see Supplementary Material Table S1 for details), N_s is the contribution fraction of *s* to NO_3^- in the PMF model results, N_{sa} is the contribution fraction of the secondary aerosol source to NO_3^- in the PMF results and ΔN_s is the contribution fraction of *s* to NO_3^- in the secondary source. ΔN_s is also regarded as the contribution fraction of *s* to OC or $PM_{2.5}$ in the secondary source, according to the sources of nitrate in secondary source, which represented the sources of overall secondary aerosol.

$$c_s = \Delta N_s \times C_{sa} + C_s \quad (3)$$

where c_s is the contribution fraction of *s* source to OC after the secondary aerosol was subdivided, C_{sa} is the contribution fraction of the secondary source to OC and C_s is the contribution of *s* to OC in the original PMF results.

$$f_s = \Delta N_s \times F_{sa} + F_s \quad (4)$$

where f_s is the contribution of *s* to $PM_{2.5}$ after the secondary aerosol was subdivided, F_{sa} is the contribution fraction of the secondary source to $PM_{2.5}$ and F_s is the contribution of *s* to $PM_{2.5}$ in the original PMF results.

2.3.4. Air Mass Back Trajectories and Potential Source Contribution Function Analysis

Air mass back trajectories: Hybrid-Single Particle Integrated Trajectories (HYSPLIT) is a professional model for analyzing the trajectories of air mass, which is a powerful tool for exploring the influence of meteorological conditions to pollutants. It was developed by the American National oceanic and atmospheric administration (NOAA) and the Australian Bureau of Meteorology and has been widely used in many studies [29,30]. In this study, TrajStat software was applied to calculate and cluster the 72h back trajectories with 3h intervals of air mass and cluster them in the sampling period [31,32].

PSCF analysis: PSCF can identify probable geographical source locations of atmospheric pollutants by combining meteorology with observed chemical pollutants, which has been widely used [30,33]. In this study, the PSCF model was applied to identify potential source regions of each source inferred from the PMF model and the 75th percentile of concentration of each source was used for the threshold criterion.

3. Results and Discussion

3.1. General Characterization of $PM_{2.5}$ and Chemical Compositions

The seasonal average $PM_{2.5}$ concentrations in Guangzhou are shown in Table 1, with annual average of 80.4 ± 30.7 μg/m^3. $PM_{2.5}$ chemical components were dominated by total carbon mass (TCM = 1.56 × OC + EC [34], 35.63%) following with SO_4^{2-} (16.29%), NO_3^- (10.18%) and NH_4^+ (8.09%)(Figure 1), which was similar with those in Beijing [35] and PRD [36]. The concentrations of SO_4^{2-}, NO_3^- and NH_4^+ all showed clear seasonal variations, being higher in winter, and lower in summer (Table 1). The mass ratio of NO_3^- to SO_4^{2-} can assess the contribution of stationary and mobile sources to $PM_{2.5}$ [3]. Generally, stationary pollution sources emit more SO_2 than NOx, such as coal-fired power plants, while mobile sources were opposite, such as vehicles [3,37]. Higher values of NO_3^-/SO_4^{2-} in winter (1.02) and spring (1.06) were similar to Beijing (1.16–1.3)[38] and the previous study of Guangzhou [39], which implied that vehicle emissions made a significant contribution to $PM_{2.5}$ in Guangzhou. The lower values of NO_3^-/SO_4^{2-} in the summer (0.42) and autumn (0.44) might be due to the increased formation of sulfate and decomposition of nitrate with high temperature and humidity, and strong solar radiation [5,35,37].

Table 1. The concentrations of chemical components in $PM_{2.5}$

Components	Autumn Mean ± Standard Deviation	Winter Mean ± Standard Deviation	Spring Mean ± Standard Deviation	Summer Mean ± Standard Deviation	Average Mean ± Standard Deviation
Organic Fractions (μg C/m³)					
OC	17.9 ± 9.3	26.2 ± 9.8	15.6 ± 5.6	10.1 ± 4.8	17.3 ± 9.6
EC	2.3 ± 1.6	3.0 ± 1.5	3.3 ± 0.9	2.9 ± 0.7	2.9 ± 1.3
OC/EC	8.58 ± 2.89	9.64 ± 3.16	4.86 ± 1.81	3.68 ± 1.93	6.69 ± 3.52
$PM_{2.5}$ and Water-Soluble Ions (μg/m³)					
$PM_{2.5}$	87.1 ± 29.3	104 ± 34.3	76.8 ± 16.7	55.4 ± 17.5	80.4 ± 30.7
SO_4^{2-}	17.0 ± 10.0	25.5 ± 7.76	9.01 ± 3.68	7.89 ± 4.77	13.5 ± 9.19
NO_3^-	5.68 ± 5.17	25.0 ± 9.41	10.3 ± 8.79	4.38 ± 8.31	9.13 ± 10.2
Cl^-	0.54 ± 0.51	1.67 ± 1.26	1.32 ± 0.75	0.49 ± 0.36	0.89 ± 0.83
NH_4^+	8.14 ± 4.11	14.02 ± 3.55	5.69 ± 2.67	3.19 ± 3.37	6.88 ± 4.88
Na^+	0.47 ± 0.29	0.44 ± 0.10	0.58 ± 0.21	0.68 ± 0.15	0.56 ± 0.23
K^+	1.01 ± 0.45	1.56 ± 0.47	0.60 ± 0.22	0.57 ± 0.20	0.85 ± 0.49
Ca^{2+}	1.92 ± 1.51	2.90 ± 0.81	1.71 ± 0.82	2.07 ± 0.54	2.05 ± 1.07
Mg^{2+}	0.18 ± 0.08	0.28 ± 0.07	0.18 ± 0.07	0.21 ± 0.07	0.20 ± 0.08
Trace Elements (ng/m³)					
Fe	652 ± 311	1030 ± 358	730 ± 316	591 ± 229	708 ± 325
As	16.4 ± 8.51	28.5 ± 11.0	9.32 ± 5.83	3.07 ± 1.58	12.4 ± 10.9
Cu	64.5 ± 68.0	61.5 ± 19.7	27.8 ± 13.4	19.9 ± 12.5	41.4 ± 43.8
Cr	18.5 ± 14.1	23.3 ± 15.2	9.67 ± 7.26	3.98 ± 2.15	12.6 ± 12.5
Mn	29. 5 ± 12.5	47.0 ± 15.6	32.7 ± 12.5	19.2 ± 6.89	29.8 ± 14.4
Ni	5.64 ± 2.85	6.62 ± 1.90	7.41 ± 2.76	4.19 ± 1.52	5.81 ± 2.60
Pb	106 ± 43.1	183 ± 51.5	47.4 ± 19.2	22.6 ± 9.92	77.1 ± 63.3
V	12.8 ± 8.72	5.55 ± 3.68	12.9 ± 4.89	7.13 ± 3.44	10.2 ± 6.32
Zn	290 ± 111	417 ± 139	175 ± 55.3	119 ± 45.7	228 ± 134

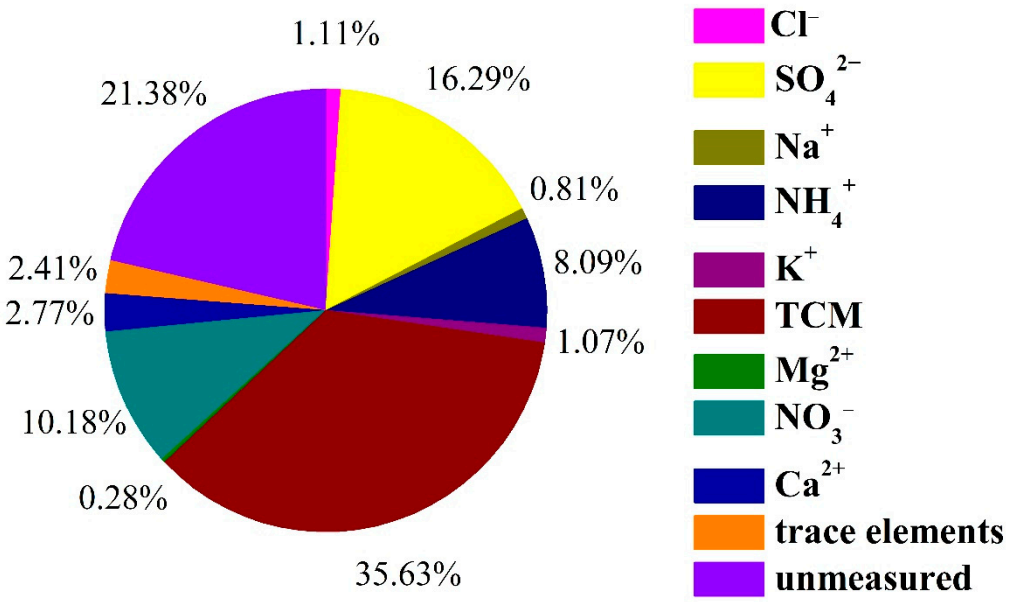

Figure 1. Contributions of chemical components to $PM_{2.5}$ mass.

The annual average mass concentrations of OC and EC were 17.3 ± 9.6 μg C/m^3 and 2.9 ± 1.3 μg C/m^3, respectively (Table 1). The seasonal variation of OC, EC and ^{14}C were described in detail in the previous study [24]. The results regarding carbonaceous aerosols in the previous study could be summarized as follows. The higher values of OC/EC in winter (9.64) and autumn (8.58) than spring (4.86) and summer (3.68) suggested that the major sources of carbonaceous aerosols changed markedly in different seasons. The stronger correlations between OC and EC in autumn (R^2 = 0.71) and winter (R^2 = 0.50), and the seasonal variation of ^{14}C indicated that biomass burning around Guangzhou, coal combustion transported from North China, and secondary organic aerosols were the main sources of carbonaceous aerosols in those two seasons. While in summer, primary emission from fossil fuels and secondary organic aerosols formation were the main sources of carbonaceous aerosols.

Trace elements contributed quite a small fraction (2.01%) to $PM_{2.5}$. However, they could provide clues of chemical species sources due to their uniqueness as tracers and stability during complex processes of atmospheric chemical reactions [40]. The levels of trace elements, including V, As, Cu, Pb and Zn, which were closely related to anthropogenic emission, were in the range of 10.2–228 ng/m^3. In this study, the concentrations of elements related to anthropogenic sources were comparable to other megacities in China [41,42] (Supplementary Material Table S2) but lower than Foshan, a major manufacturing center, which had many heavily polluting factories. Compared with the past observed data, the levels of V, As, Cu, Pb and Zn in Guangzhou showed a declining trend, probably resulting from more strict regulations on the trace elements emission from industry. It implied that industry might not have been the dominating source of $PM_{2.5}$ in Guangzhou since 2014.

3.2. Source Apportionment Results

Source apportionment based on PMF results**:** Combining with the bootstrapping and displacement technique (Table S3), Q values (Figure S1), scaled residuals and source profile, a seven-factor solution was chosen. Then the most physically reasonable results were obtained with seven factors after constraints were run with radiocarbon data. The source profiles identified by the PMF model are shown in Figure 2, the temporal series of each source contribution to $PM_{2.5}$ is displayed in Figure 3, and the contribution of each source to $PM_{2.5}$ mass concentration is shown in Figure 4.

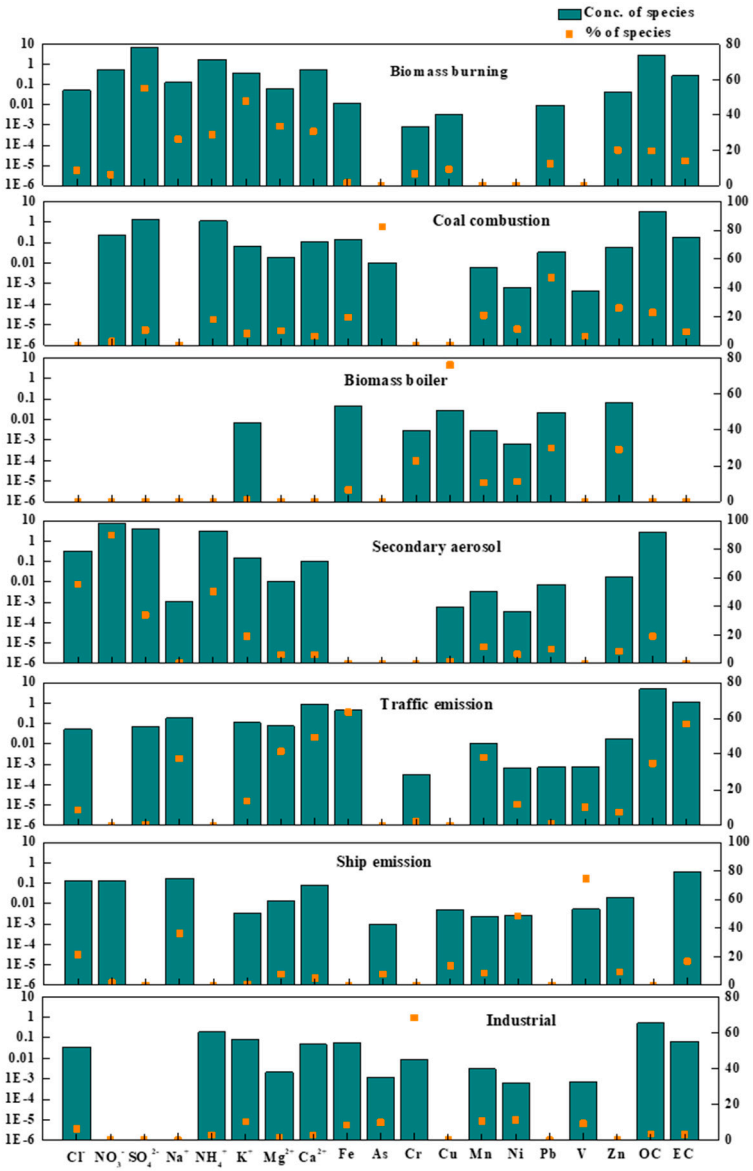

Figure 2. Source profiles of seven sources identified by the PMF model (concentration units: μg/m^3).

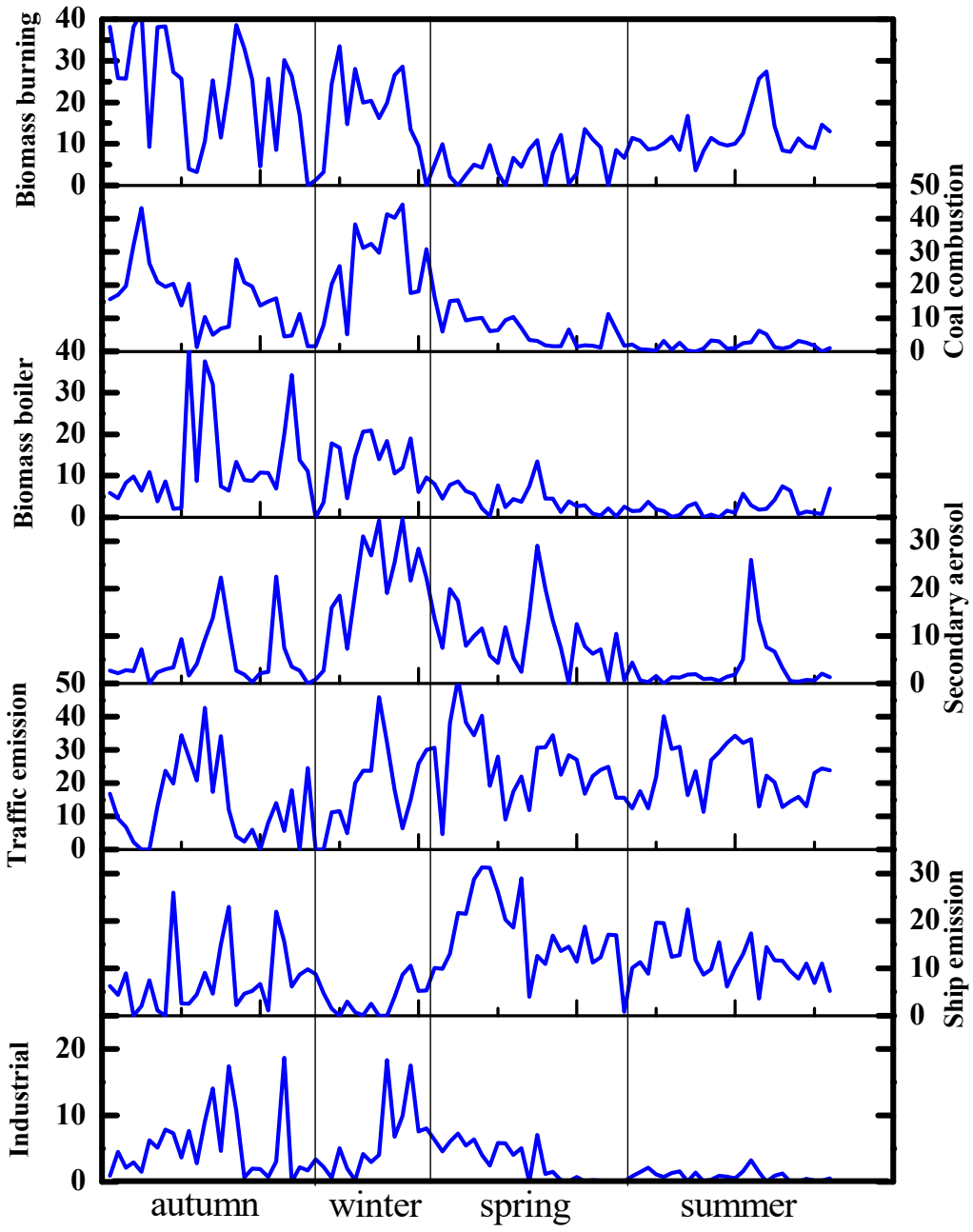

Figure 3. Temporal series of each source contribution to $PM_{2.5}$ (μg/m^3).

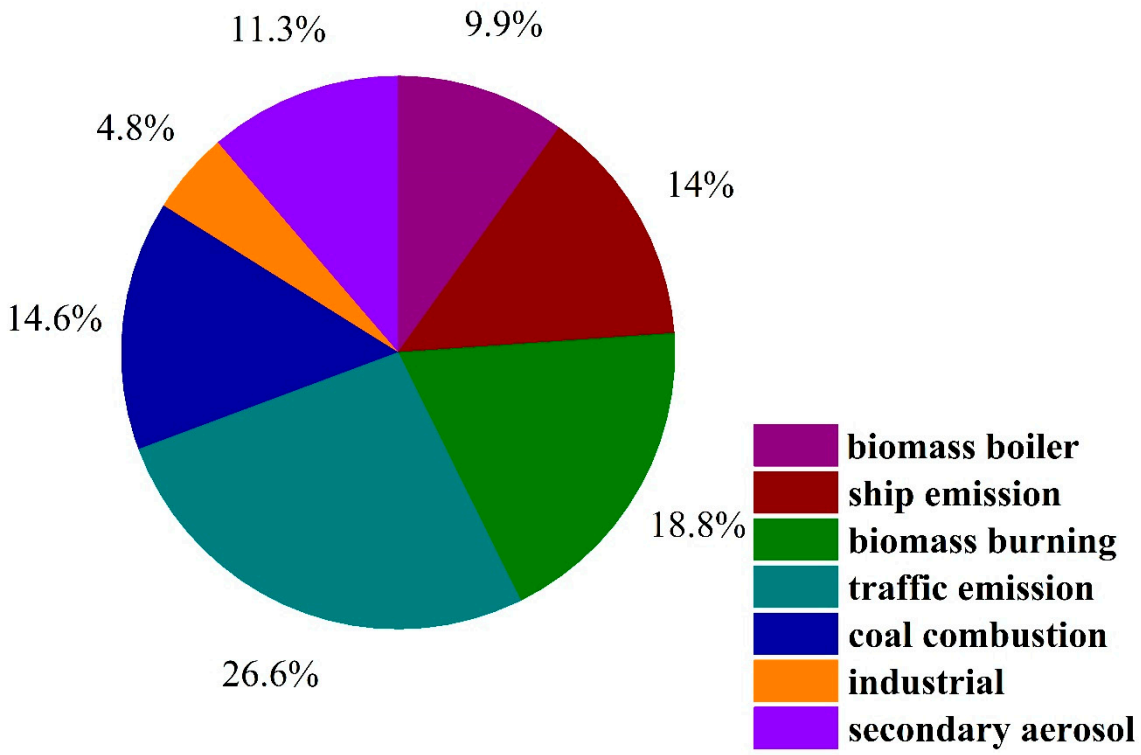

Figure 4. Contributions of each source to $PM_{2.5}$ mass concentration.

The first source represented biomass burning accounting for 18.8% of $PM_{2.5}$ mass, which was characterized by a high level of K^+, SO_4^{2-}, NH_4^+, OC and EC. It showed a similar profile with biomass burning especially a high concentration of K^+ [4,11,43-46]. In the suburbs of Guangzhou, biomass was widely used for cooking [5]. In addition, the contribution of this source to $PM_{2.5}$ was obviously higher in autumn and winter than in spring and summer, which may be affected by transportation from North China. The average ratio of OC/EC in this source was 7.23 ± 2.69, which further implied biomass burning.

The second source was coal combustion, typically identified by high level of As followed by Pb, Zn, OC and EC, accounting for 14.6% of $PM_{2.5}$ mass. In Guangdong Province, coal is the major energy for the generation of commercial, factories and residential electric power [5]. Furthermore, coal combustion emits a high level of As, Pb and Zn [1,47-50]. In Guangdong Province, coal combustion was the dominant emission contributor for As (48%), there was a relatively lower contribution to Pb (7%), and this was reflected in the high concentration of OC and EC [5,51].

The third source was assigned as a biomass boiler, reflected in high concentrations of Fe, K^+, Cu, Pb, Zn and Mn, accounting for 9.9% of $PM_{2.5}$ mass. In 2015, the number of industrial companies who used a biomass boiler was 2032, accounting for 30% of the total number of industrial companies and second only to a coal-fired boiler in Guangdong province [52]. Efficient combustion of the biomass boiler resulted mainly in inorganic particles and heavy metal, including K, S, Cl, Zn, Ca, Na, Fe, Mn, Cu and Pb [52-54]. Hence, the third source was identified by biomass boiler emission.

The fourth source was secondary aerosol, which was mainly composed by NO_3^-, NH_4^+, Cl^- and SO_4^{2-}. Generally, secondary nitrate in the atmosphere was generated by gaseous pollutants such as nitrogen oxide [5]. The high contribution of SO_4^{2-} in this source implied the secondary formation of sulfate [11]. In total, secondary aerosol accounted for 11.3% of $PM_{2.5}$ mass.

The fifth source was rich in EC, OC, Fe, Al, Mn, Ca^{2+}, Mg^{2+} and Na^+. EC in this source accounted for almost half of EC in $PM_{2.5}$; what is more, vehicle emission was usually characterized by high loading of EC [11]. High level of Fe, Ca^{2+}, Na^+ and Mg^{2+} were also found in the Zhujiang tunnel experiment about fine particles from on-road vehicles [55]. Na^+ in this source may indicate that the

re-suspension of particles from sea salt deposited on the road [55]. Fe, Al, Ca^{2+}, Mg^{2+} and Mn are major components of crustal, which may be re-suspended from a road caused by fleeting vehicles [55-57]. In addition, vehicles are an important source of Fe in particles due to the wear of engines and brakes [45]. Vehicles emitting Ca^{2+} and Mg^{2+} may also result from the combustion of additives [55,58]. The fifth source was inferred as traffic emission, accounting for 26.6% of $PM_{2.5}$ mass.

The sixth source was ship emission and typically characterized by a high level of V, Ni and Na^{+}, accounting for 14.0% of $PM_{2.5}$ mass. V and Ni in the atmosphere are chiefly from fossil fuel combustion, especially heavy oil and crude oil, which is often attributed to ship emission [4,45,59]. Moreover, the ratio of V/Ni more than 0.7 is a sign of $PM_{2.5}$ affected by ship emission [46]. The average ratio of V/Ni from the observed data was 1.63 ± 0.59 suggesting a significant contribution from ship emissions to $PM_{2.5}$. In addition, the contribution of Na^{+} was also high in this source implying the influence of seaports, which further verified that the sixth source was ship emission.

The seventh source depicted industrial emission and contributed 4.8% to $PM_{2.5}$ mass with a high level of Cr. Cr in the atmosphere mainly originated from industry and coal combustion [49]. It was worth noting that the iron and steel industry was the dominant source of Cr accounting for 82% Cr emission in Guangdong Province [51]. In Guangdong province, approximately 34.15 million tons of steel were produced from 2013 to 2014, as shown in Guangdong province statistical data (http://stats.gd.gov.cn/), which potentially had a strong impact on Cr in the atmosphere. In addition, other industries also emitted Cr, such as electroplating, leather tanning and the textile industry [60]. Thus, the seventh source was interpreted as industrial emission.

The temporal series of each source contribution to $PM_{2.5}$ in PMF results suggested that biomass burning was enhanced in autumn and winter (Figure 3), revealing the impact of intensive biofuel combustion in local regions and transportation from the north in those two seasons. The 72h back trajectories were clustered and the results are displayed in Figure S2a,b in the Supplementary Material. Traffic emission showed no obvious seasonal variation due to heavy traffic all year round in Guangzhou. Coal combustion peaked in winter potentially resulting from transportation with the prevailing north wind. While ship emissions were enhanced in spring and summer with the prevailing south wind from the South China Sea. The industrial and biomass boiler showed relatively high contributions during autumn and winter, which might result from the washout by rainfall in spring and summer or more transportation from the north in winter [36]. In short, the seasonal variation of primary sources identified by the PMF model was reasonable.

Source apportionment based on PMF combined with Bayesian model results**:** Typically, secondary aerosol accounts for a large proportion of $PM_{2.5}$ in China [1], the contributions of diverse sources to secondary aerosol also need to be estimated to make effective regulatory measures. However, source apportionment of secondary aerosol generally cannot be resolved by receptor models [10,61]. In this study, secondary aerosol contributed 11.3% to $PM_{2.5}$, a relatively high contribution. Based on the Bayesian mixing model, the source of NO_3^- was attributed to coal combustion, traffic emission and biogenic source. Secondary aerosol sources identified by PMF were subdivided into three sources (coal combustion, traffic emission and biogenic source) according to the discrepancy in source apportionment of NO_3^- between PMF and the Bayesian mixing model results. In the secondary source identified by PMF, the relatively high correlations between NO_3^- and $PM_{2.5}$ ($R^2 = 0.869$, $p < 0.01$), OC ($R^2 = 0.863$, $p < 0.01$), SO_4^{2-} ($R^2 = 0.726$, $p < 0.01$), respectively, were found in this study. Assuming the sources of secondary aerosol are almost the same as those of its main components, the sources of nitrate in the secondary source were used to represent the sources of overall secondary aerosol. Hence, secondary aerosol identified by PMF could also be subdivided into primary sources according to the discrepancy in source apportionment of NO_3^- between the PMF and Bayesian mixing model results. After secondary aerosols were assigned, the contributions of the three sources to $PM_{2.5}$ were calculated according to Equations (2) and (4), and results were displayed in Figure 5.

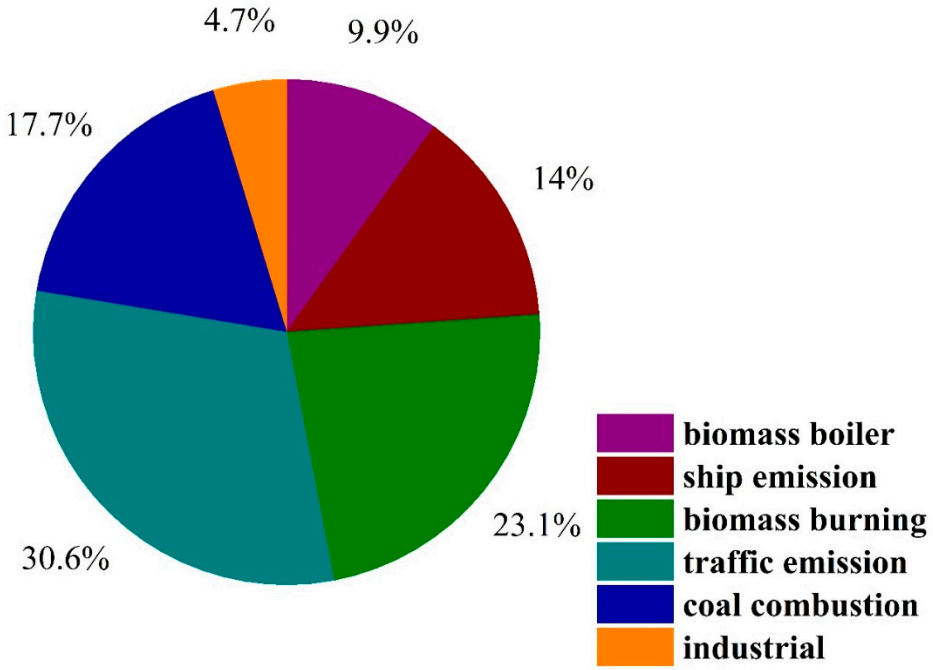

Figure 5. Contributions of each source to $PM_{2.5}$ mass concentration after subdividing secondary aerosols.

After secondary aerosols were assigned, the four dominant contributors to $PM_{2.5}$ were traffic emission (30.6%), biomass burning (23.1%), coal combustion (17.7%) and ship emission (14.0%). The sources related to industrial processes, including industrial emission and biomass boiler, accounted for 14.6% of $PM_{2.5}$. According to the information released by the environmental protection bureau of Guangdong province, from 2013 to 2014, the main source of $PM_{2.5}$ was vehicle exhaust, whose contribution was 21.7%, followed by coal combustion (20.6%) and industrial source (11.5%)[62] (http://gdee.gd.gov.cn/). In 2017, Tao et al.[2] used the PMF model for source apportionment to $PM_{2.5}$ and reported that ship emission, coal combustion and biomass burning were the prominent contributors to $PM_{2.5}$ in Guangzhou. In 2017, Zhou et al.[63] applied the CMB model for source apportionment to $PM_{2.5}$ and suggested that vehicle emission was the major source (14–21%) of $PM_{2.5}$ in PRD. In addition, $PM_{2.5}$ sources in the PRD region were estimated according to an emission inventory in a similar period and were compared with our study. The dominant contributors to $PM_{2.5}$ in PRD were road mobile source (23.76%), power plants (17.68%), industrial sources including industrial combustion (13.78%) and industrial process (12.11%), biomass burning (11.49%)[64]. The $PM_{2.5}$ emission sources between Guangzhou and PRD were similar. In summary, the $PM_{2.5}$ source categories in Guangzhou and their contributions resolved by diverse methods were slightly different since tracers for identifying a specific source were not unique and many methods did not have a unique solution [10]. However, the major sources of $PM_{2.5}$ in this study were similar to previous studies mentioned above.

3.3. Performance Assessment of Source Apportionment Results

Source apportionment assessment based on original PMF results: Carbonaceous species generally originate from different sources with diverse fossil/non-fossil fractions. Therefore, ^{14}C analysis of OC and EC provides more information for source apportionment [15,16]. Comparing the contributions of fossil/non-fossil sources to OC and EC inferred from ^{14}C measurements with the corresponding results of PMF could assess source apportionment results. Based on the source types identified by PMF, traffic emission, coal combustion, ship emission and industrial emission were classified as fossil sources, biomass burning was classified in non-fossil sources, and secondary aerosol source was not classified. The source contributions of OC and EC after classification were

calculated according to Equation (1). The comparison results between ^{14}C measurements and the PMF model are shown in Figure 6.

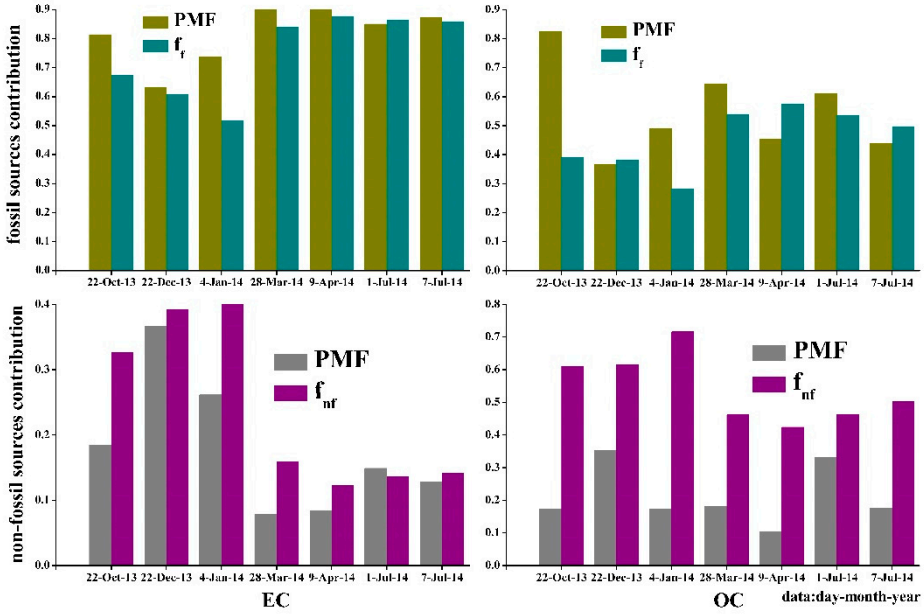

Figure 6. Comparison of the source contribution to EC and OC classified from the PMF results and the corresponding ^{14}C measurements (f_f and f_{nf} were fossil and non-fossil sources contribution to carbon species inferred from ^{14}C measurements, respectively).

The variation in seasonal contribution to EC displayed by PMF was similar with the ^{14}C results, except for three days when the non-fossil source contribution to EC in PMF results were slightly lower than ^{14}C results. For OC, the difference between PMF and ^{14}C results was more significant than EC. It might be attributed to the sources of OC being more complex than EC. EC is generated directly from the incomplete combustion of fossil fuel and biomass, and often used as a primary emission source tracer [16]. However, OC cannot only be emitted from primary sources (primary organic carbon) but can also be generated by the oxidation reaction of gas-phase compounds in the atmosphere (secondary organic carbon, SOC).

Source apportionment assessment after assignment of secondary aerosols: To accurately compare the difference in the contribution of non-fossil sources to OC between PMF and ^{14}C results, OC in secondary aerosol sources was also subdivided into three sources (coal combustion, traffic emission and biogenic source). After secondary aerosols were subdivided, the contributions of the three sources to OC in PMF results were calculated according to Equations (2) and (3). Then, the contribution of non-fossil sources to OC inferred from ^{14}C measurements were compared with PMF results again as shown in Figure 7.

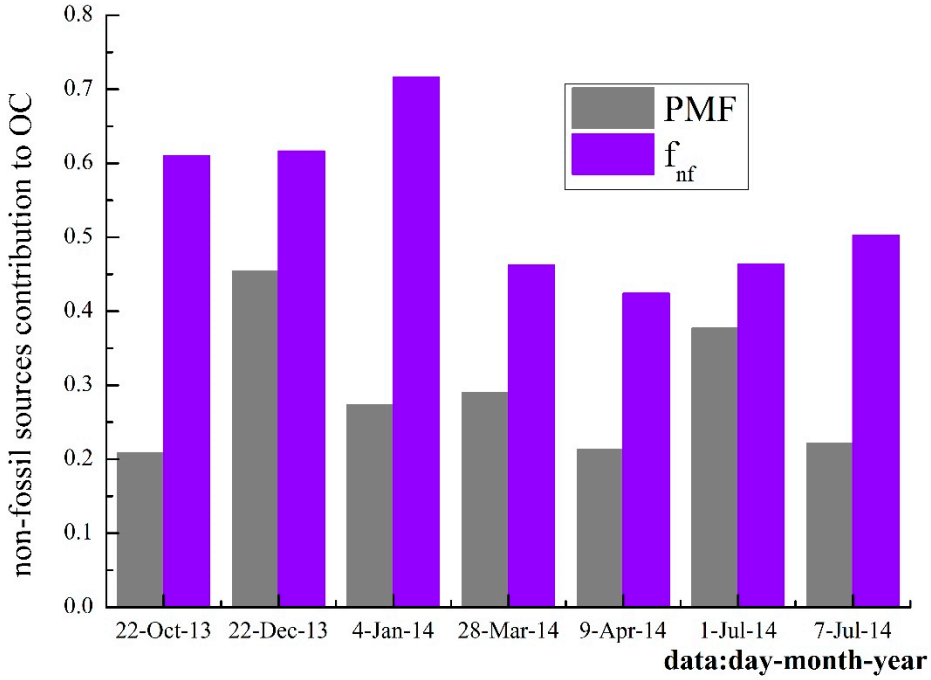

Figure 7. Non-fossil source contributions of OC after secondary aerosol subdivision and the corresponding ^{14}C fractions.

After secondary aerosol sources were assigned, the gap of non-fossil source contribution to OC between PMF and ^{14}C results narrowed. However, the non-fossil source contribution to OC in PMF results was still lower than ^{14}C results. The significant contribution of biogenic secondary organic aerosol (BSOA) to non-fossil source organic aerosol has been suggested by previous studies. In 2017, Zhang et al.[65] indicated that non-fossil sources (such as biogenic SOC and biomass burning) were dominant contributors of OC in Beijing. In 2019, Miyakawa et al.[66] found that the contributions of non-fossil sources except biomass burning, which may have originated from natural sources including terrestrial and oceanic biogenic sources, to OC were substantial in the Asian outflow region. However, the formation of BSOA might be influenced by anthropogenic sources [67]. In 2014, Matsui et al.[67] found the formation of BSOA was enhanced by anthropogenic NOx, VOCs and primary organic aerosol (POA) because they increased the oxidation rates of VOCs, the concentrations of precursor VOCs and the gas–particle partitioning ratios of organic compounds. The great majority of BSOA (78%) was formed through the influence of anthropogenic sources over East Asia [67]. In 2007, Weber et al.[68] reported that the WSOC contained 70–80% of modern carbon in Atlanta. Nevertheless, the WSOC showed a spatial correlation with tracers of vehicle emission, which suggested that precursors of anthropogenic emissions were the key to control the generation of organic aerosol. In this study, the non-fossil source contribution to OC in PMF results was lower than ^{14}C measurements. This might because OC generated by the reaction between Biogenic VOCs and precursors released from fossil fuels was attributed to fossil sources.

Overall, the comparison suggested that the PMF model running with seven factors provided a reliable source apportionment to $PM_{2.5}$ in Guangzhou. The PMF model captured the primary sources well, implied by the comparison results of EC between modeled data and ^{14}C measurements. However, the PMF model was deficient for identifying biogenic source due to the lack of organic molecular markers suggested by the gap of OC between modeled data and ^{14}C measurements. The comparison results also implied that SOC from biogenic sources potentially had different formation pathways through anthropogenic precursors and should be considered in the PMF results. In addition, the contribution of biogenic SOC could not be determined accurately and would be partially grouped into fossil source contribution. For improving $PM_{2.5}$ source apportionment, organic molecular tracers should be utilized to identify biogenic source. The significance of applying biogenic

secondary organic aerosol tracers would be even greater in regions with high plant coverage and relatively high BSOA contributions.

3.4. PSCF Results

PSCF analysis was conducted to identify potential source regions of $PM_{2.5}$ using the time series of each source contribution to $PM_{2.5}$ in PMF results after secondary aerosol subdivision, and the results were displayed in Supplementary Material Figure S3. PSCF results suggested that biomass burning mainly took place in the local region, North China and the South China Sea. In the potential source region, the South China Sea, biomass burning was maybe affected by an air mass from the Indo-China Peninsula (ICP), where biomass burning events were intensive [30,69]. Then, PSCF based on 120 h back trajectories of air mass were calculated, which indicated that the air mass of the sampling site passed through ICP. North China and the local region were the potential source regions of coal combustion, biomass boiler and industrial emission. For ship emissions, the coastal regions of Guangdong Province and the South China Sea were potential source areas. It is worth mentioning that Guangzhou ports were among the top-ten largest ports in the world [2], which might have a significant influence on $PM_{2.5}$. Traffic emission was mainly contributed to by the local region and was affected by sea salt partly, which coincided with the discussion in Section 3.2.

4. Conclusions

Guangzhou, a rapidly developing city in South China, had suffered from $PM_{2.5}$ pollution with complex sources. In this study, $PM_{2.5}$ average mass concentration was 80.4 ± 30.7 μg/cm^3 and was dominated by TCM (35.63%) and SO_4^{2-} (16.29%). The PMF and Bayesian mixing models were applied in source apportionment to $PM_{2.5}$. The results indicated that traffic emission (30.6%), biomass burning (23.1%), coal combustion (17.7%) and ship emissions (14.0%) were dominant in $PM_{2.5}$ mass concentrations. Traffic emission was mainly contributed to by the local region. Biomass burning took place in local regions, North China and the ICP. North China and local regions were the potential source regions of coal combustion. Ship emissions were affected by the coastal regions of Guangdong Province and the South China Sea.

Source apportionment results were assessed by comparing fossil/non-fossil source contributions to OC and EC inferred from ^{14}C measurements with the corresponding results in PMF. There was no significant difference in EC between modeled data and measurements, indicating that the PMF model captured the primary sources well. However, due to the lack of organic molecular markers, the PMF model was deficient for identifying biogenic source implied by the discrepancy of OC between modeled data and measurements. OC from the non-fossil source was underestimated in PMF results, suggesting that SOC related to biogenic sources might be classed into fossil sources. This study suggested that SOC from biogenic sources perhaps had various formation pathways through anthropogenic precursors and should be considered in PMF results. Furthermore, the contribution of biogenic SOC could not be resolved exactly and would be partly grouped into fossil source contribution. In future research, the utility of the organic molecular markers in source apportionment to identify biogenic source is particularly noteworthy, especially for the places with high vegetation coverage and strong biogenic SOA contributions.

There is no doubt that the source apportionment of $PM_{2.5}$ from 2013 to 2014 may be lagging on the current conditions to some extent. Nevertheless, this period is the beginning of a large-scale pollution abatement in China. This study can provide background reference for the implementation effect of $PM_{2.5}$ control [20]. Moreover, the method of combining the PMF and Bayesian models for source apportionment of $PM_{2.5}$ and tracing the primary emission source of secondary aerosols can be instructive for related studies in the future.

Supplementary Materials: The following are available online at www.mdpi.com/2073-4433/11/5/512/s1, Text S1: Chemical composition analysis; Text S2: Research methods; Text S3: Bayesian mixing model; Text S4: PMF model results and uncertainty estimation. Table S1: Contributions of three sources to NO_3^- resolved by Bayesian mixing model (%); Table S2: Comparison of trace elements in $PM_{2.5}$ in representative cities; Table S3**:** Percentage of BS factors assigned to each base case factor with a correlation threshold of 0.6. Figure S1: The changes of Q

values from base model runs with factors from five to nine; Figure S2: 72h back trajectories in **a**) winter/ **b**) summer sampling period; Figure S3: Potential source regions of each factor. (a: biomass burning, b: biomass burning 120h, c: traffic emission, d: ship emission, e: coal combustion, f: biomass boiler, g: industrial).

Author Contributions: Methodology, J.L., C.T., D.C., Z.Z. and G.Z.; validation, J.L., C.T., T.L., H.J., D.C., Z.Z. and G.Z.; formal analysis, J.L., C.T., T.L., H.J. and Z.Z.; data curation, J.L.; writing—original draft preparation, T.L. and J.L.; writing—review and editing, T.L and J.L. All authors have read and agreed to the published version of the manuscript.

Funding: This work was funded by the National Key R&D Program of China (2017YFC0212000), Natural Science Foundation of China (41473101 and 41977177), Guangdong Basic and Applied Basic Research Foundation (2019A1515011175) and Guangdong Foundation for Program of Science and Technology Research (Grant No. 2017B030314057).

Acknowledgments: We sincerely acknowledge for the technical support provided by Kong Yang and Zeyu Sun, and acknowledge Ben Liu, Qing Zhang, and Refayat Nigar for polishing up English in this paper.

Conflicts of Interest: The authors declare that they have no conflict of interest or personal relationships that could have appeared to influence the work reported in this paper.

References

1. Huang, R.J.; Zhang, Y.; Bozzetti, C.; Ho, K.F.; Cao, J.J.; Han, Y.; Daellenbach, K.R.; Slowik, J.G.; Platt, S.M.; Canonaco, F., et al. High secondary aerosol contribution to particulate pollution during haze events in China. *Nature* **2014**, *514*, 218-222, doi:10.1038/nature13774.
2. Tao, J.; Zhang, L.; Cao, J.; Zhong, L.; Chen, D.; Yang, Y.; Chen, D.; Chen, L.; Zhang, Z.; Wu, Y., et al. Source apportionment of PM2.5 at urban and suburban areas of the Pearl River Delta region, south China - With emphasis on ship emissions. *Sci. Total Environ.* **2017**, *574*, 1559-1570, doi:10.1016/j.scitotenv.2016.08.175.
3. Zong, Z.; Wang, X.; Tian, C.; Chen, Y.; Qu, L.; Ji, L.; Zhi, G.; Li, J.; Zhang, G. Source apportionment of $PM_{2.5}$ at a regional background site in North China using PMF linked with radiocarbon analysis: insight into the contribution of biomass burning. *Atmos. Chem. Phys.* **2016**, *16*, 11249-11265, doi:10.5194/acp-16-11249-2016.
4. Yu, L.; Wang, G.; Zhang, R.; Zhang, L.; Song, Y.; Wu, B.; Li, X.; An, K.; Chu, J. Characterization and Source Apportionment of $PM_{2.5}$ in an Urban Environment in Beijing. *Aerosol Air Qual. Res.* **2013**, *13*, 574-583, doi:10.4209/aaqr.2012.07.0192.
5. Song, Y.; Dai, W.; Wang, X.; Cui, M.; Su, H.; Xie, S.; Zhang, Y. Identifying dominant sources of respirable suspended particulates in Guangzhou, China. *Environ. Eng. Sci.* **2008**, *25*, 959-968, doi:10.1089/ees.2007.0146.
6. Ni, T.; Han, B.; Bai, Z. Source Apportionment of PM_{10} in Four Cities of Northeastern China. *Aerosol Air Qual. Res.* **2012**, *12*, 571-582, doi:10.4209/aaqr.2011.12.0243.
7. Zhang, Y.; Zheng, M.; Cai, J.; Hu, Y.; G., R.A.; Wang, X.; Wang, S.; Zhang, Y. Comparison and overview of $PM_{2.5}$ source apportionment methods (in Chinese). *Chin. Sci. Bull.* **2015**, *60*, 109-121, doi:10.1360/N972014-00975.
8. Hopke, P.K. Review of receptor modeling methods for source apportionment. *J. Air Waste Manage. Assoc.* **2016**, *66*, 237-259, doi:10.1080/10962247.2016.1140693.
9. Mooibroek, D.; Schaap, M.; Weijers, E.P.; Hoogerbrugge, R. Source apportionment and spatial variability of $PM_{2.5}$ using measurements at five sites in the Netherlands. *Atmos. Environ.* **2011**, *45*, 4180-4191, doi:10.1016/j.atmosenv.2011.05.017.
10. Zhu, Y.; Huang, L.; Li, J.; Ying, Q.; Zhang, H.; Liu, X.; Liao, H.; Li, N.; Liu, Z.; Mao, Y., et al. Sources of particulate matter in China: Insights from source apportionment studies published in 1987-2017. *Environ. Int.* **2018**, *115*, 343-357, doi:10.1016/j.envint.2018.03.037.

11. Huang, X.; Yun, H.; Gong, Z.; Li, X.; He, L.; Zhang, Y.; Hu, M. Source apportionment and secondary organic aerosol estimation of $PM_{2.5}$ in an urban atmosphere in China. *Sci. China Earth Sci.* **2013**, *57*, 1352-1362, doi:10.1007/s11430-013-4686-2.
12. Zhang, Y.; Cai, J.; Wang, S.; He, K.; Zheng, M. Review of receptor-based source apportionment research of fine particulate matter and its challenges in China. *Sci. Total Environ.* **2017**, *586*, 917-929, doi:10.1016/j.scitotenv.2017.02.071.
13. Zong, Z.; Wang, X.; Tian, C.; Chen, Y.; Fang, Y.; Zhang, F.; Li, C.; Sun, J.; Li, J.; Zhang, G. First Assessment of NOx Sources at a Regional Background Site in North China Using Isotopic Analysis Linked with Modeling. *Environ. Sci. Technol.* **2017**, *51*, 5923-5931, doi:10.1021/acs.est.6b06316.
14. Yuan, Z.B.; Yu, J.Z.; Lau, A.K.H.; Louie, P.K.K.; Fung, J.C.H. Application of positive matrix factorization in estimating aerosol secondary organic carbon in Hong Kong and its relationship with secondary sulfate. *Atmos. Chem. Phys.* **2006**, *6*, 25–34.
15. Zhang, Y.L.; Li, J.; Zhang, G.; Zotter, P.; Huang, R.J.; Tang, J.H.; Wacker, L.; Prevot, A.S.; Szidat, S. Radiocarbon-based source apportionment of carbonaceous aerosols at a regional background site on Hainan Island, South China. *Environ. Sci. Technol.* **2014**, *48*, 2651-2659, doi:10.1021/es4050852.
16. Liu, J.; Li, J.; Zhang, Y.; Liu, D.; Ding, P.; Shen, C.; Shen, K.; He, Q.; Ding, X.; Wang, X., et al. Source apportionment using radiocarbon and organic tracers for $PM_{2.5}$ carbonaceous aerosols in Guangzhou, South China: contrasting local- and regional-scale haze events. *Environ. Sci. Technol.* **2014**, *48*, 12002-12011, doi:10.1021/es503102w.
17. Lu, X.; Chen, Y.; Huang, Y.; Lin, C.; Li, Z.; Fung, J.C.H.; Lau, A.K.H. Differences in concentration and source apportionment of $PM_{2.5}$ between 2006 and 2015 over the PRD region in southern China. *Sci. Total Environ.* **2019**, *673*, 708-718, doi:10.1016/j.scitotenv.2019.03.452.
18. Wang, X.; Bi, X.; Sheng, G.; Fu, J. Chemical composition and sources of PM10 and PM2.5 aerosols in Guangzhou, China. *Environ. Monit. Assess.* **2006**, *119*, 425-439, doi:10.1007/s10661-005-9034-3.
19. Wang, J.; Ho, S.S.H.; Ma, S.; Cao, J.; Dai, W.; Liu, S.; Shen, Z.; Huang, R.; Wang, G.; Han, Y. Characterization of $PM_{2.5}$ in Guangzhou, China: uses of organic markers for supporting source apportionment. *Sci. Total Environ.* **2016**, *550*, 961-971, doi:10.1016/j.scitotenv.2016.01.138.
20. Zong, Z.; Tan, Y.; Wang, X.; Tian, C.; Li, J.; Fang, Y.; Chen, Y.; Cui, S.; Zhang, G. Dual-modelling-based source apportionment of NOx in five Chinese megacities: Providing the isotopic footprint from 2013 to 2014. *Environ. Int.* **2020**, *137*, 105592, doi:10.1016/j.envint.2020.105592.
21. Liu, D.; Li, J.; Cheng, Z.; Zhong, G.; Zhu, S.; Ding, P.; Shen, C.; Tian, C.; Chen, Y.; Zhi, G., et al. Sources of non-fossil-fuel emissions in carbonaceous aerosols during early winter in Chinese cities. *Atmos. Chem. Phys.* **2017**, *17*, 11491–11502, doi:10.5194/acp-17-11491-2017.
22. Zhang, Y.L.; Perron, N.; Ciobanu, V.G.; Zotter, P.; Minguillón, M.C.; Wacker, L.; Prévôt, A.S.H.; Baltensperger, U.; Szidat, S. On the isolation of OC and EC and the optimal strategy of radiocarbon-based source apportionment of carbonaceous aerosols. *Atmos. Chem. Phys.* **2012**, *12*, 10841-10856, doi:10.5194/acp-12-10841-2012.
23. Zhang, Y.L.; Huang, R.J.; El Haddad, I.; Ho, K.F.; Cao, J.J.; Han, Y.; Zotter, P.; Bozzetti, C.; Daellenbach, K.R.; Canonaco, F., et al. Fossil vs. non-fossil sources of fine carbonaceous aerosols in four Chinese cities during the extreme winter haze episode of 2013. *Atmos. Chem. Phys.* **2015**, *15*, 1299-1312, doi:10.5194/acp-15-1299-2015.

24. Liu, D.; Vonwiller, M.; Li, J.; Liu, J.; Szidat, S.; Zhang, Y.; Tian, C.; Chen, Y.; Cheng, Z.; Zhong, G. Fossil and Non-fossil Fuel Sources of Organic and Elemental Carbon Aerosols in Beijing, Shanghai and Guangzhou: Seasonal Carbon-source Variation. *Aerosol Air Qual. Res.* **2020**, *submitted*.
25. McIlvin, M.R.; Altabet, M.A. Chemical Conversion of Nitrate and Nitrite to Nitrous Oxide for Nitrogen and Oxygen Isotopic Analysis in Freshwater and Seawater *Anal. Chem.* **2005**, *77*, 5589-5595.
26. Paatero, P.; Tapper, U. Analysis of different modes of factor analysis as least squares fit problems. *Chemometrics Intell. Lab. Syst.* **1993**, *18*, 183-194.
27. Paatero, P.; Hopke, P.K.; Song, X.H.; Ramadan, a.Z. Understanding and controlling rotations in factor analytic models. *Chemometrics Intell. Lab. Syst.* **2002**, *60*, 253-264.
28. Parnell, A.C.; Phillips, D.L.; Bearhop, S.; Semmens, B.X.; Ward, E.J.; Moore, J.W.; Jackson, A.L.; Grey, J.; Kelly, D.J.; Inger, R. Bayesian stable isotope mixing models. *Environmetrics* **2013**, 10.1002/env.2221, n/a-n/a, doi:10.1002/env.2221.
29. Zong, Z.; Chen, Y.; Tian, C.; Fang, Y.; Wang, X.; Huang, G.; Zhang, F.; Li, J.; Zhang, G. Radiocarbon-based impact assessment of open biomass burning on regional carbonaceous aerosols in North China. *Sci. Total Environ.* **2015**, *518-519*, 1-7, doi:10.1016/j.scitotenv.2015.01.113.
30. Geng, X.; Zhong, G.; Li, J.; Cheng, Z.; Mo, Y.; Mao, S.; Su, T.; Jiang, H.; Ni, K.; Zhang, G. Molecular marker study of aerosols in the northern South China Sea: Impact of atmospheric outflow from the Indo-China Peninsula and South China. *Atmos. Environ.* **2019**, *206*, 225-236, doi:10.1016/j.atmosenv.2019.02.033.
31. Wang, Y.Q.; Zhang, X.Y.; Draxler, R.R. TrajStat: GIS-based software that uses various trajectory statistical analysis methods to identify potential sources from long-term air pollution measurement data. *Environ. Modell. Softw.* **2009**, *24*, 938-939, doi:10.1016/j.envsoft.2009.01.004.
32. Li, Y.; An, X.; Fan, G. Transport pathway and potential source area of atmospheric particulates in Beijing (in Chinese). *Chin. Environ. Sci.* **2019**, *39*, 915-927.
33. Jain, S.; Sharma, S.K.; Choudhary, N.; Masiwal, R.; Saxena, M.; Sharma, A.; Mandal, T.K.; Gupta, A.; Gupta, N.C.; Sharma, C. Chemical characteristics and source apportionment of $PM_{2.5}$ using PCA/APCS, UNMIX, and PMF at an urban site of Delhi, India. *Environ. Sci. Pollut. Res.* **2017**, *24*, 14637-14656, doi:10.1007/s11356-017-8925-5.
34. Srinivas, B.; Sarin, M.M. $PM_{2.5}$, EC and OC in atmospheric outflow from the Indo-Gangetic Plain: temporal variability and aerosol organic carbon-to-organic mass conversion factor. *Sci. Total Environ.* **2014**, *487*, 196-205, doi:10.1016/j.scitotenv.2014.04.002.
35. Huang, X.; Liu, Z.; Zhang, J.; Wen, T.; Ji, D.; Wang, Y. Seasonal variation and secondary formation of size-segregated aerosol water-soluble inorganic ions during pollution episodes in Beijing. *Atmos. Res.* **2016**, *168*, 70-79, doi:10.1016/j.atmosres.2015.08.021.
36. Huang, X.-F.; Zou, B.-B.; He, L.-Y.; Hu, M.; Prévôt, A.S.H.; Zhang, Y.-H. Exploration of $PM_{2.5}$ sources on the regional scale in the Pearl River Delta based on ME-2 modeling. *Atmos. Chem. Phys.* **2018**, *18*, 11563-11580, doi:10.5194/acp-18-11563-2018.
37. Wang, Y.; Zhuang, G.; Tang, A.; Yuan, H.; Sun, Y.; Chen, S.; Zheng, A. The ion chemistry and the source of $PM_{2.5}$ aerosol in Beijing. *Atmos. Environ.* **2005**, *39*, 3771-3784, doi:10.1016/j.atmosenv.2005.03.013.
38. Wu, X.; Chen, B.; Wen, T.; Habib, A.; Shi, G. Concentrations and chemical compositions of PM_{10} during hazy and non-hazy days in Beijing. *J. Environ. Sci. (China)* **2020**, *87*, 1-9, doi:10.1016/j.jes.2019.03.021.
39. Liu, Z.; Gao, W.; Yu, Y.; Hu, B.; Xin, J.; Sun, Y.; Wang, L.; Wang, G.; Bi, X.; Zhang, G., et al. Characteristics of $PM_{2.5}$ mass concentrations and chemical species in urban and background areas of China: emerging

results from the CARE-China network. *Atmos. Chem. Phys.* **2018**, *18*, 8849-8871, doi:10.5194/acp-18-8849-2018.

40. Tan, J.; Duan, J.; Ma, Y.; He, K.; Cheng, Y.; Deng, S.X.; Huang, Y.L.; Si-Tu, S.P. Long-term trends of chemical characteristics and sources of fine particle in Foshan City, Pearl River Delta: 2008-2014. *Sci. Total Environ.* **2016**, *565*, 519-528, doi:10.1016/j.scitotenv.2016.05.059.
41. Yang, F.; Tan, J.; Zhao, Q.; Du, Z.; He, K.; Ma, Y.; Duan, F.; Chen, G.; Zhao, Q. Characteristics of $PM_{2.5}$ speciation in representative megacities and across China. *Atmos. Chem. Phys.* **2011**, *11*, 5207-5219, doi:10.5194/acp-11-5207-2011.
42. Ming, L.; Jin, L.; Li, J.; Fu, P.; Yang, W.; Liu, D.; Zhang, G.; Wang, Z.; Li, X. $PM_{2.5}$ in the Yangtze River Delta, China: Chemical compositions, seasonal variations, and regional pollution events. *Environ. Pollut.* **2017**, *223*, 200-212, doi:10.1016/j.envpol.2017.01.013.
43. Li, X.H.; Wang, S.X. Particulate and Trace Gas Emissions from Open Burning of Wheat Straw and Corn Stover in China. *Environ. Sci. Technol.* **2007**, *41*, 6052-6058.
44. Zou, B.-B.; Huang, X.-F.; Zhang, B.; Dai, J.; Zeng, L.-W.; Feng, N.; He, L.-Y. Source apportionment of $PM_{2.5}$ pollution in an industrial city in southern China. *Atmos. Pollut. Res.* **2017**, *8*, 1193-1202, doi:10.1016/j.apr.2017.05.001.
45. Dall; amp; apos; Osto, M.; Querol, X.; Amato, F.; Karanasiou, A.; Lucarelli, F.; Nava, S.; Calzolai, G., et al. Hourly elemental concentrations in $PM_{2.5}$ aerosols sampled simultaneously at urban background and road site during SAPUSS – diurnal variations and PMF receptor modelling. *Atmos. Chem. Phys.* **2013**, *13*, 4375-4392, doi:10.5194/acp-13-4375-2013.
46. Wang, X.; Zong, Z.; Tian, C.; Chen, Y.; Luo, C.; Li, J.; Zhang, G.; Luo, Y. Combining Positive Matrix Factorization and Radiocarbon Measurements for Source Apportionment of $PM_{2.5}$ from a National Background Site in North China. *Sci. Rep.* **2017**, *7*, doi:10.1038/s41598-017-10762-8.
47. Tan, J.H.; Duan, J.C.; Ma, Y.L.; Yang, F.M.; Cheng, Y.; He, K.B.; Yu, Y.C.; Wang, J.W. Source of atmospheric heavy metals in winter in Foshan, China. *Sci. Total Environ.* **2014**, *493*, 262-270, doi:10.1016/j.scitotenv.2014.05.147.
48. Duan, J.; Tan, J. Atmospheric heavy metals and Arsenic in China: Situation, sources and control policies. *Atmos. Environ.* **2013**, *74*, 93-101, doi:10.1016/j.atmosenv.2013.03.031.
49. Cheng, K.; Wang, Y.; Tian, H.; Gao, X.; Zhang, Y.; Wu, X.; Zhu, C.; Gao, J. Atmospheric emission characteristics and control policies of five precedent-controlled toxic heavy metals from anthropogenic sources in China. *Environ. Sci. Technol.* **2015**, *49*, 1206-1214, doi:10.1021/es5037332.
50. Chen, L.; Zhou, S.; Wu, S.; Wang, C.; He, D. Concentration, fluxes, risks, and sources of heavy metals in atmospheric deposition in the Lihe River watershed, Taihu region, eastern China. *Environ. Pollut.* **2019**, *255*, 113301, doi:10.1016/j.envpol.2019.113301.
51. Sha, Q.; Lu, M.; Huang, Z.; Yuan, Z.; Jia, G.; Xiao, X.; Wu, Y.; Zhang, Z.; Li, C.; Zhong, Z., et al. Anthropogenic atmospheric toxic metals emission inventory and its spatial characteristics in Guangdong province, China. *Sci. Total Environ.* **2019**, *670*, 1146-1158, doi:10.1016/j.scitotenv.2019.03.206.
52. Zhang, J.; Li, M.; Cheng, C.; Cheng, p.; Bai, L.; Liu, J.; Zhou, Y.; Huang, B. Mass spectral features of fine particles from biomass boilers (in Chinese). *Environ. Pollut. Control* **2018**, *40*, 1167-1174.
53. Bäfver, L.S.; Leckner, B.; Tullin, C.; Berntsen, M. Particle emissions from pellets stoves and modern and old-type wood stoves. *Biomass Bioenergy* **2011**, *35*, 3648-3655, doi:10.1016/j.biombioe.2011.05.027.
54. Tissari, J.; Hytönen, K.; Sippula, O.; Jokiniemi, J. The effects of operating conditions on emissions from masonry heaters and sauna stoves. *Biomass Bioenergy* **2009**, *33*, 513-520, doi:10.1016/j.biombioe.2008.08.009.

55. He, L.-Y.; Hu, M.; Zhang, Y.-H.; Huang, X.-F.; Yao, T.-T. Fine Particle Emissions from On-Road Vehicles in the Zhujiang Tunnel, China. *Environ. Sci. Technol.* **2008**, *42*, 4461–4466.
56. Liu, J.; Wu, D.; Fan, S.; Mao, X.; Chen, H. A one-year, on-line, multi-site observational study on water-soluble inorganic ions in $PM_{2.5}$ over the Pearl River Delta region, China. *Sci. Total Environ.* **2017**, *601*, 1720-1732, doi:10.1016/j.scitotenv.2017.06.039.
57. Masiol, M.; Hopke, P.K.; Felton, H.D.; Frank, B.P.; Rattigan, O.V.; Wurth, M.; LaDuke, G.H. Analysis of major air pollutants and submicron particles in New York City and Long Island. *Atmos. Environ.* **2017**, *148*, 203-214, doi:10.1016/j.atmosenv.2016.10.043.
58. Cadle, S.H.; Mulawa, P.A.; Ball, J.; Donase, C.; Weible, A.; Sagebiel, J.C.; Knapp, K.T.; Snow, R. Particulate Emission Rates from In-Use High-Emitting Vehicles Recruited in Orange County,California. *Environ. Sci. Technol.* **1997**, *31*, 3405-3412.
59. Zhao, Y.; Feng, L.; Shang, B.; Li, J.; Lv, G.; Wu, Y. Pollution Characterization and Source Apportionment of Day and Night $PM_{2.5}$ Samples in Urban and Suburban Communities of Tianjin (China). *Arch. Environ. Contam. Toxicol.* **2019**, *76*, 591-604, doi:10.1007/s00244-019-00614-z.
60. Hu, Y.; Cheng, H. Application of stochastic models in identification and apportionment of heavy metal pollution sources in the surface soils of a large-scale region. *Environ. Sci. Technol.* **2013**, *47*, 3752-3760, doi:10.1021/es304310k.
61. Wang, Q.; Huang, X.H.H.; Tam, F.C.V.; Zhang, X.; Liu, K.M.; Yeung, C.; Feng, Y.; Cheng, Y.Y.; Wong, Y.K.; Ng, W.M., et al. Source apportionment of fine particulate matter in Macao, China with and without organic tracers: A comparative study using positive matrix factorization. *Atmos. Environ.* **2019**, *198*, 183-193, doi:10.1016/j.atmosenv.2018.10.057.
62. Li, Y.-y.; Ge, C. Research progress of $PM_{2.5}$ source analysis in three main regions of China (in Chinese). *Mod. Chem. Ind.* **2017**, *37*, 1-5, doi:10.16606 /j.cnk.issn0253-4320.2017.04.001.
63. Zhou, J.; Xiong, Y.; Xing, Z.; Deng, J.; Du, K. Characterizing and sourcing ambient $PM_{2.5}$ over key emission regions in China II: Organic molecular markers and CMB modeling. *Atmos. Environ.* **2017**, *163*, 57-64, doi:10.1016/j.atmosenv.2017.05.033.
64. Yang, J. A study on refining temporal and spatial allocation for the 2012-based on air pollution emission inventory in the Pearl River Delta region (in chinese). South China University of Technology, 2015.
65. Zhang, Y.; Ren, H.; Sun, Y.; Cao, F.; Chang, Y.; Liu, S.; Lee, X.; Agrios, K.; Kawamura, K.; Liu, D., et al. High Contribution of Nonfossil Sources to Submicrometer Organic Aerosols in Beijing, China. *Environ. Sci. Technol.* **2017**, *51*, 7842-7852, doi:10.1021/acs.est.7b01517.
66. Miyakawa, T.; Komazaki, Y.; Zhu, C.; Taketani, F.; Pan, X.; Wang, Z.; Kanaya, Y. Characterization of carbonaceous aerosols in Asian outflow in the spring of 2015: Importance of non-fossil fuel sources. *Atmos. Environ.* **2019**, *214*, doi:10.1016/j.atmosenv.2019.116858.
67. Matsui, H.; Koike, M.; Kondo, Y.; Takami, A.; Fast, J.D.; Kanaya, Y.; Takigawa, M. Volatility basis-set approach simulation of organic aerosol formation in East Asia: implications for anthropogenic–biogenic interaction and controllable amounts. *Atmos. Chem. Phys.* **2014**, *14*, 9513-9535, doi:10.5194/acp-14-9513-2014.
68. Weber, R.J.; Sullivan, A.P.; Peltier, R.E.; Russell, A.; Yan, B.; Zheng, M.; de Gouw, J.; Warneke, C.; Brock, C.; Holloway, J.S., et al. A study of secondary organic aerosol formation in the anthropogenic-influenced southeastern United States. *J. Geophys. Res.* **2007**, *112*, doi:10.1029/2007jd008408.
69. Yadav, I.C.; Linthoingambi Devi, N.; Li, J.; Syed, J.H.; Zhang, G.; Watanabe, H. Biomass burning in Indo-China peninsula and its impacts on regional air quality and global climate change-a review. *Environ. Pollut.* **2017**, *227*, 414-427, doi:10.1016/j.envpol.2017.04.085.